

# PROTON STRUCTURE IMPACT ON SENSITIVITY TO EXTRA-DIMENSIONS AT LHC

S. FERRAG

*ATLAS Collaboration*

*Laboratoire de Physique Nucléaire et des hautes Energies, Paris, France*



The LHC data will provide sensitivity to an unification of the couplings at low energies in the range  $\sim 10$ -100 TeV. It is demonstrated in this note that the lack of knowledge on the proton structure, specifically its gluon distribution, can lower dramatically the sensitivity of bare cross section measurements to this physics. However, some more elaborated strategies could probably be developed to recover an important part of the sensitivity.

## 1 Introduction

Theoretical particle physics deals with three fundamental energy scales: the electroweak breaking scale at  $\approx 10^2$  GeV, the grand unification theory (GUT) scale at  $\approx 10^{16}$  GeV and the Planck scale, where gravitation becomes as strong as the other interactions, at  $\approx 10^{19}$  GeV. Those three scales are separated by a troubling physical energy range in which the Standard Model (SM) predicts no new physics. This forms the well known hierarchy problem. A new framework has been recently proposed to adress this problem<sup>1,2</sup>. Related models contain only one fundamental scale, which can be as low as few TeV, and a more complex space-time structure with  $\delta$  new compactified spacial dimensions. In this picture, the Standard Model matter fields are localised in a (3+1) dimensional hyperplane (3-brane). The above scales become effective and can be expressed as functions of the fundamental scale and the compactification radius of the extra-dimensions<sup>1</sup>. This new picture induces interesting phenomenological aspects at the LHC if the fundamental scale is as low as a few TeV (10-100 TeV): production of gravitons and observation of Kaluza Klein (KK) excitations will be possible if the radius size of one of the  $\delta$  compactified extra-dimensions is about a few TeV. If gauge bosons can propagate in the extra-dimensions, we also expect a violation of the SM logarithmic behaviour of the running couplings<sup>4,3</sup>. This

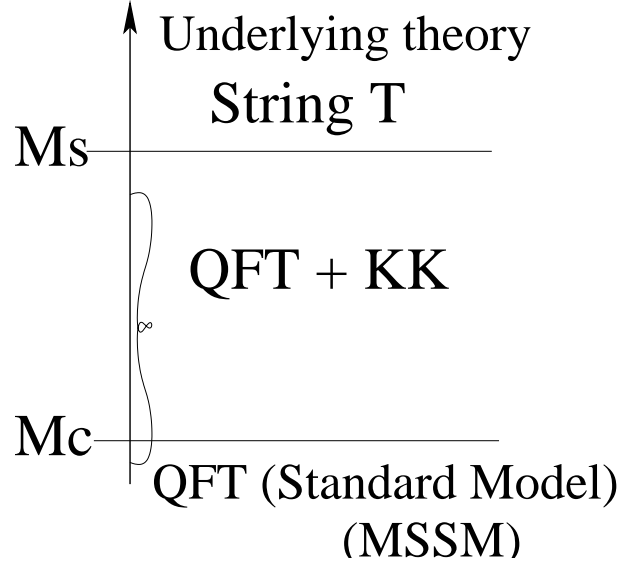


Figure 1: *In the transition region between the underlying theory scale around the string scale  $M_s$  and the Standard Model scale below the compactification scale  $M_c$ , the underlying theory is approached with a Quantum Field Theory (QFT) including the KK excitation. The validity region of calculation given in references [3,4] extends up to this transition region.*

note will concentrate on this latter aspect. LHC data will provide a measurement of the different couplings on a large energy range and allow for experimental sensitivity to a possible non SM running. Following reference<sup>5</sup>, the measurement of  $\alpha_S$  is investigated by looking at the di-jets cross section.

In this analysis, the di-jets cross section in the presence of extra-dimensions is studied and QCD aspects of this measurement are investigated. Extra-dimensions affect this cross section through the  $\alpha_S$  evolution. This new  $\alpha_S$  running is given in references<sup>3,4</sup>. Kaluza Klein excitations are included only in the  $\alpha_S$  running through the  $\beta$  coefficients in the Renormalization Group Equations (RGE). The explicit exchange of these excitations is not taken into account in the calculation of the di-jets cross section.

A preliminary work on the sensitivity to extra-dimensions at the LHC, using di-jets production<sup>5</sup>, shows that the sensitivity to extra-dimensions at LHC reaches 5 to 10 TeV in compactification scale following the  $\alpha_S$  running scenario (see below).

A complementary analysis using the Monte Carlo techniques is presented here: a first step consisted in the implementation of the new  $\alpha_S$  running in the event generator Pythia 6.152. As the di-jets production will be done over a large Pt range, the impact of Parton Density Function (PDF) uncertainties in the proton on the sensitivity of the di-jets cross section to Standard Model RGE violations is investigated. This is done using PDFs from CTEQ6 that come with 40 PDF sets. This framework enables, for the first time, to investigate rigourously the impact of the PDF uncertainties on a given measurement. The results are then expressed in terms of an impact of the proton structure on the extra-dimensions sensitivity.

## 2 Event Generation

The di-jets cross section in the extra-dimensions regime is assumed to be a continuity of the Standard Model di-jets cross section with a new  $\alpha_S$  running. This can be written as:

$$\frac{d\sigma^{XD}}{dM_{JJ}} = \frac{d\sigma^{SM}}{dM_{JJ}}(\alpha_s^{XD}), \quad (1)$$

where  $\sigma^{XD}$  and  $\alpha_s^{XD}$  are respectively, the cross section and the strong coupling in presence of extra-dimensions and  $\sigma^{SM}$  is the cross section computed within the Standard Model.  $M_{JJ}$  is the di-jets invariant mass.

The implemented model is inspired from references<sup>3,4</sup>. We assume that the underlying theory has  $3+\delta$  independent space dimensions and one time dimension. The  $\delta$  extra-dimensions are compactified on a hypersphere of radius  $R_c$ . In this theory all the fundamental scales are close to the weak scale and standard gauge bosons propagate in the extra-dimensions. The compactification scale  $M_c$  is between two scales

$$M_{Z^0} \lesssim M_c = 1/R_c \lesssim M_{string} = \mathcal{O}(100 \text{ TeV}). \quad (2)$$

Following<sup>3,4</sup>, we assume that in the TeV energy range the theory can be well approximated by a field theory formulated in a 4-dimensional space-time (figure 1). In these papers, the field theory is assumed to be the Minimal Supersymmetric Standard Model (MSSM) whose RGE have no sensitive difference with the Standard Model ones at few TeV scale<sup>a</sup>. In this study, the field theory is supposed to be the Standard Model. Consequently, no supersymmetric particles are put in the physical spectrum, only  $\alpha_S$  MSSM running is used. The presence of the KK excitations of the gluons, photons,  $Z^0$  and  $W^\pm$  affects the renormalization evolution of the gauge coupling by power-law type corrections. At the lowest order, the scale dependence of the gauge couplings is given by<sup>3,4</sup>:

$$\alpha_i^{-1}(\mu) = \alpha_i^{-1}(\mu_0) - \frac{b_i - \tilde{b}_i}{2\pi} \ln \frac{\mu}{\mu_0} - \frac{\tilde{b}_i}{4\pi} \int_{r\mu^{-2}}^{r\mu_0^{-2}} \frac{dt}{t} \left[ \vartheta_3 \left( \frac{it}{\pi R_c^2} \right) \right]^\delta, \quad (3)$$

where  $i = 1, 2, 3$  labels the gauge groups of the MSSM, and the coefficients of the usual one loop beta functions:

$$(b_1, b_2, b_3) = (33/5, 1, -3), \quad (4)$$

are supplemented by new contributions from the properly supersymmetrized KK excitations

$$(\tilde{b}_1, \tilde{b}_2, \tilde{b}_3) = (3/5, -3, -6) + \eta (4, 4, 4), \quad (5)$$

where  $\eta$  is the number of chiral fermions in the theory and set to be  $\eta = 0$  for simplicity. In the last term of Eq. (3)  $\vartheta_3$  denotes the elliptic Jacobi function and

$$r = \pi (X_\delta)^{-2/\delta} \quad \text{with} \quad X_\delta = \frac{2\pi^{\delta/2}}{\delta\Gamma(\delta/2)}. \quad (6)$$

The power-law term in Eq. (3) accelerates the running of the gauge couplings and makes them meet earlier than the usual unification scale of  $\approx 10^{16}$  GeV. In particular, for  $\eta = 0$ , the strong coupling decreases faster than what the logarithmic running describes.

---

<sup>a</sup>The difference of the gauge evolutions between the Standard Model and the MSSM is negligible compared to the effect of an  $\mathcal{O}(\text{TeV})$  size extra dimension in the  $\mu = 1\text{-}10$  TeV range. Keeping in agreement with References<sup>3,4</sup>, the MSSM beta functions are used.

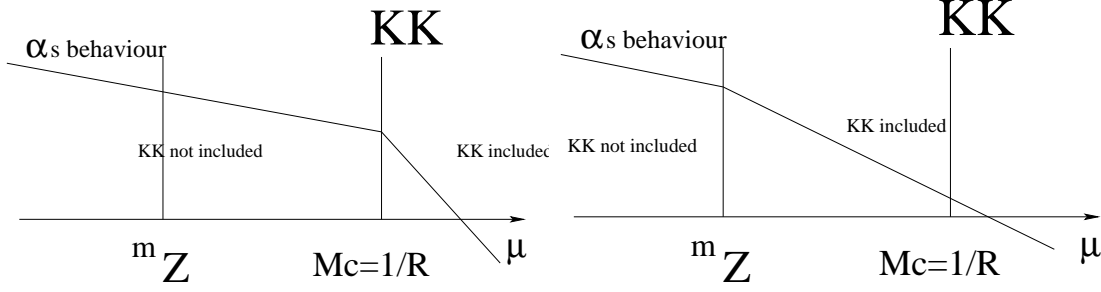


Figure 2: (Left) pessimistic scenario: the matching between the Standard Model running of  $\alpha_S$  and the new running is performed at the KK mass. This doesn't take into account the KK width. (Right) optimistic scenario: the matching between the two  $\alpha_S$  runnings is performed at the  $Z^0$  mass. The KK width is overestimated. The matching at the KK threshold is discussed in details in reference[6].

### 2.1 Implementation of $\alpha_S$

Following<sup>5</sup>, the transition between the usual Standard Model running and the modified running can be done within two extreme scenarios, the so called pessimistic and optimistic ones (figure 2). The pessimistic case assumes that the running is altered only above  $\mu = 1/R_c$ . The optimistic scenario assumes that the asymptotic high energy region formula can be downscaled to the  $Z^0$  mass in Eq. (3). A correct treatment of the transition should take into account Kaluza Klein width effects which are large as  $\Gamma_n = 2\alpha_S(Q)n/R_c^b$ . Some theoretical work is ongoing to treat this problem properly. In this note, only the pessimistic scenario is implemented in Pythia 6.152 and used in this analysis in a conservative way.

Preliminary results on the sensitivity to extra-dimensions given in<sup>5</sup> show that the sensitivity to extra-dimensions reaches 5 TeV (10 TeV) in compactification scale using the pessimistic (optimistic) prescription. Moreover, these results depend very smoothly on the number of extra-dimensions<sup>c</sup>.

Figure (3) shows the implemented running for different extra-dimensions parameters ( $\delta, M_c$ ). The values of the implemented compactification scale  $M_c$  vary from 2 to 14 TeV and 2, 4 and 6 for the numbers of extra-dimensions  $\delta$ . Below a given value of  $M_c$ , we can see the MSSM logarithmic running of  $\alpha_S$  and the extra-dimensions corrected one above  $M_c$ . Figure (3.a) shows for  $\delta = 2$  extra-dimensions and for different compactification scales the  $\alpha_S$  running among the energy scale. figure (3.b) shows  $\alpha_S$  running for  $\delta = 6$  extra-dimensions.

### 2.2 Di-jets cross section in presence of extra-dimensions

Once the extra-dimensions  $\alpha_S$  running is implemented, di-jet events are simulated within the ATLAS fast simulation framework. Because of the strong decreasing behaviour of the cross section, events are generated in the Pt range 500-5000 GeV by step of  $\Delta Pt = 500$  GeV. The lower Pt limit  $Pt_{min}$  is varied as:

$$Pt_{min} = 500 \cdot i \text{ GeV}, \quad i = 1 \text{ to } 10. \quad (7)$$

10 000 events are generated for each extra-dimensions parameter ( $\delta, M_c$ ) and for each Pt bin.

<sup>b</sup>For example: the width of a 10 TeV resonance is about 2 TeV.

<sup>c</sup>For  $M_c = 5$  TeV, the separation between the Standard Model prediction and the extra-dimensions prediction is in order of  $5\sigma$  independently from the number of extra-dimensions.

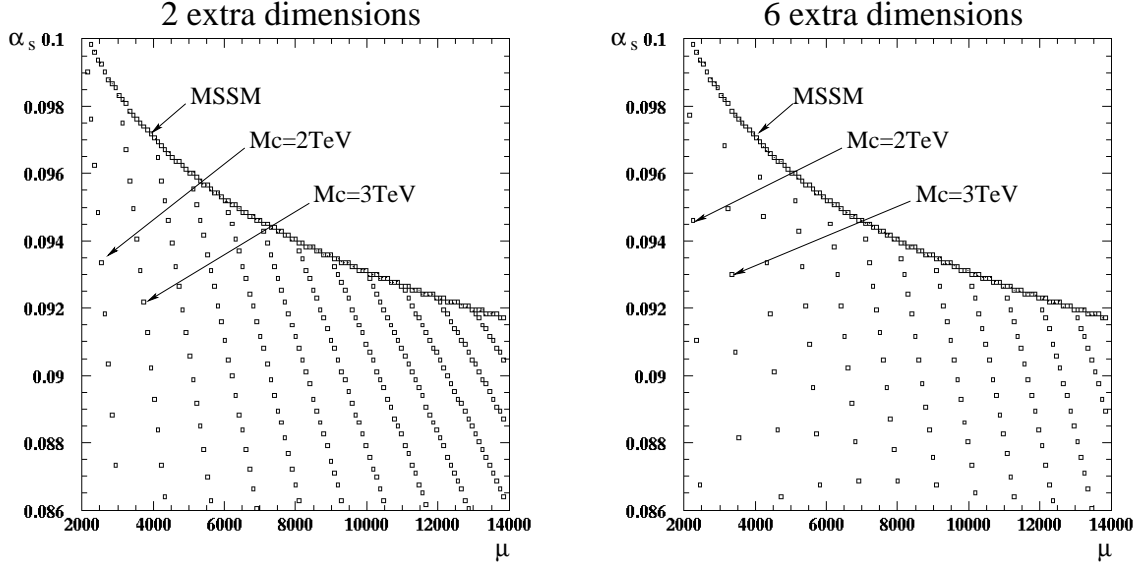


Figure 3: Implemented  $\alpha_s$  running for  $\delta = 2$  (left) and  $\delta = 6$  extra-dimensions (right). The upper line corresponds to the MSSM logarithmic running. Every going-down line corresponds to new running for a given compactification scale. This latter vary from  $M_c=2$  to  $14$  TeV. For a given value of  $M_c$ , the considered  $\alpha_s$  running is composed by the MSSM part below  $M_c$  and the new part above  $M_c$  with the pessimistic scenario matching at  $M_c$ .

Figures (4) and (5) compare the di-jets cross section, as a function of  $P_t$ , for different extra-dimensions parameters to the Standard Model prediction. Figure (4) presents di-jet cross sections according to the number of extra-dimensions ( $\delta = 2$  and  $\delta = 6$ ) and figure (5) presents them according to the compactification scales ( $M_c=2$  and  $M_c=8$  TeV). The Standard Model di-jets cross section prediction is presented in black and the extra-dimensions model prediction in green or red. For a given number of extra-dimensions, predictions for different values of the compactification scales  $M_c$  are presented in figure (4). One can notice a very unusual effect from this new physics since extra-dimensions existence reduces the di-jets cross section whereas most other new physics models predict an increase of the cross section through new particle exchange. Note also that this cancellation effect becomes stronger for low compactification scale values. For high compactification scale values, the theory tends to the Standard Model prediction (figure (5)). The effect above becomes more important when the number of the extra-dimensions increases as shown in figure (4) for  $\delta = 6$ .

### 3 Di-jets cross section and proton structure uncertainties

#### 3.1 Introduction

The goal of this section is to estimate the impact of the proton structure uncertainties on the total di-jets cross section. Thus, QCD effects have to be understood in order to estimate the realistic discovery power of new physics in that channel.

The di-jet cross section using the factorization theorem can be written as:

$$\sigma = \sum_{ij} \int f_i(Q^2, x_i) f_j(Q^2, x_j) \sigma_{i+j \rightarrow 2} d x_i d x_j, \quad (8)$$

where  $\sigma_{i+j \rightarrow 2}$  is the partonic cross section of the di-jet process  $parton_i + parton_j \rightarrow parton +$

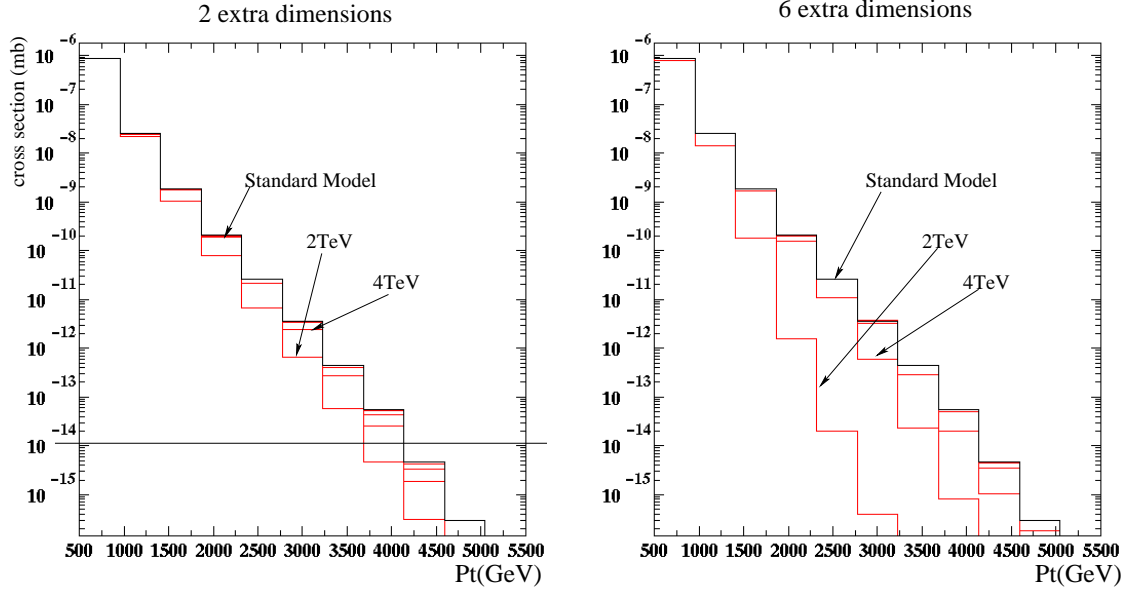


Figure 4: *di-jets cross section predictions for  $\delta = 2$  ( $\delta=6$ ) extra-dimensions at left (at right). The horizontal line shows the limit corresponding to the first year of LHC high luminosity, ie,  $100 \text{ fb}^{-1}$ . All the extra-dimensions predictions are below the Standard Model one. The separation between the predictions increases with the number of extra-dimensions .*

*parton*. It is calculable at given order in perturbation theory.  $f_i(Q^2, x_i)$  is the Parton Density Function which gives the probability of finding a parton  $i$  in the proton carrying a fraction  $x_i$  of its momentum.  $Q^2$  is the center of mass energy.

PDF models with intrinsic errors became available in Jan 2002. The CTEQ collaboration recently introduced a new scheme giving access to evaluate them. The CTEQ6 PDFs<sup>7</sup>. We implemented this new framework in Pythia 6.152 before the LHAPDF<sup>8</sup> interface was public.

CTEQ6 contains 3 different versions;

- CTEQ6D: fitted using Deep Inelastic Scattering (DIS) data (BCDMS, H1, ZEUS, NMC, CCFR, E608 and E866),
- CTEQ6L: based on Leading Order (LO) calculations and fitted on the the above data adding the Tevatron ones,
- CTEQ6M: based on NLO calculations and fitted on the same CTEQ6L data, only this version includes the uncertainties calculations.

CTEQ6 fit is based on the Hessian method. This enables a characterization of parton parametrization in the neighbourhood of the global  $\chi^2$  minimum and, then gives access to the uncertainty calculation. This latter is given as follows<sup>7</sup>:

- a global fit on the data above is performed using 20 free parameters. This gives the nominal PDF set CTEQ6M. The obtained global  $\chi^2$  is about 1954 for 1811 data points.
- the global  $\chi^2$  is increased by  $\Delta\chi^2 = 100$  to get the error matrix.
- this matrix is diagonalized to get 20 eigenvectors corresponding to 20 independent directions in the parameter space.

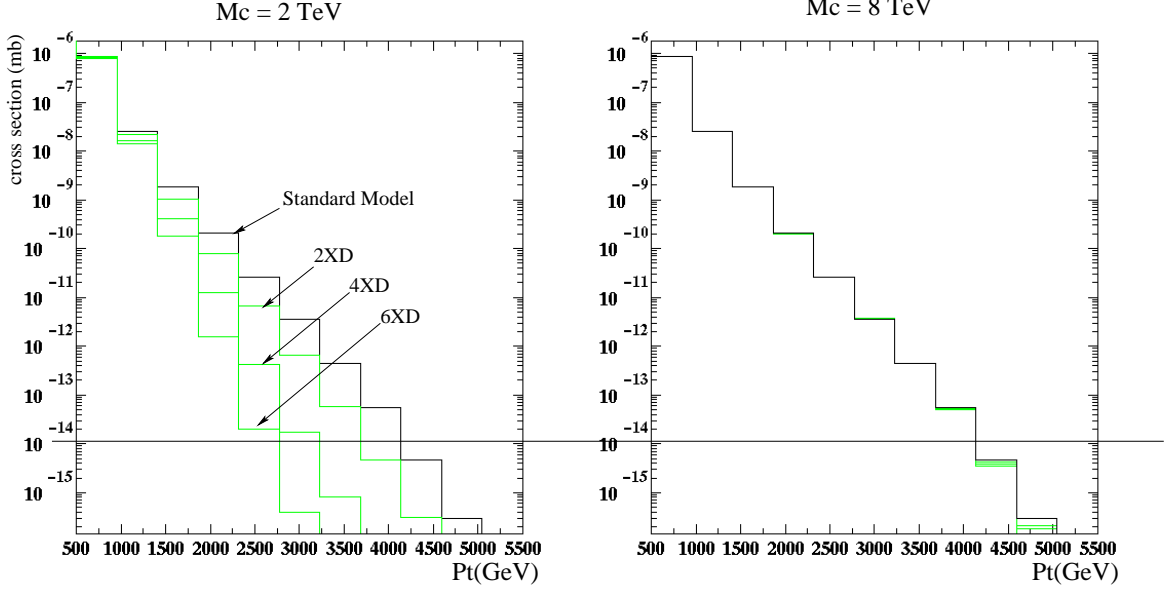


Figure 5: *di-jet cross section predictions with compactification scale  $M_c=2$  TeV at left and  $M_c=8$  TeV at right. For high  $M_c$  values, extra-dimensions predictions tend to the Standard Model one.*

- for every eigenvector, up and down excursions are performed in the tolerance gap. This gives 40 sets of new parameters corresponding to 40 new sets of PDFs. These are used in the uncertainty calculations and are called *error PDFs* for simplicity.

Extra-dimensions sensitivity is calculated by comparing extra-dimension model predictions to the Standard Model one. As a side product, the Standard Model prediction zone which contains the Standard Model cross section uncertainty zone is obtained.

### 3.2 Standard Model Prediction

Let  $S_0$  be the PDF set corresponding to the nominal fit, *ie*, CTEQ6M.  $S_i$  is the set of the error PDFs with  $i$  from 1 to 40.  $\sigma_0$  is the di-jet cross section nominal prediction (here, the Standard Model prediction) and  $\sigma_i = \sigma(S_i)$  are the cross sections computed using  $S_i$ . We use  $\Delta\sigma_i^+ = \sigma_i - \sigma_0$  when  $\sigma_i > \sigma_0$  and  $\Delta\sigma_i^- = \sigma_i - \sigma_0$  when  $\sigma_i < \sigma_0$ . The uncertainties are summed quadratically to define  $\Delta\sigma^\pm = \sqrt{\sum_i \sigma_i^\pm}$ . The di-jets cross section as predicted by the Standard Model and its uncertainties is fixed by:

$$\sigma_{0-\Delta\sigma^-}^{+\Delta\sigma^+}$$

and is shown in figure (6) for one and three standard deviations.

It is interesting to notice that every measured di-jet cross section in this zone is explained within the Standard Model by a simple new PDF fit. This interpretation means also that *in this zone, every power of discovering new physics is killed and absorbed by a PDF fit*. One expects a reduction of the sensitivity to extra-dimensions because of these uncertainties.

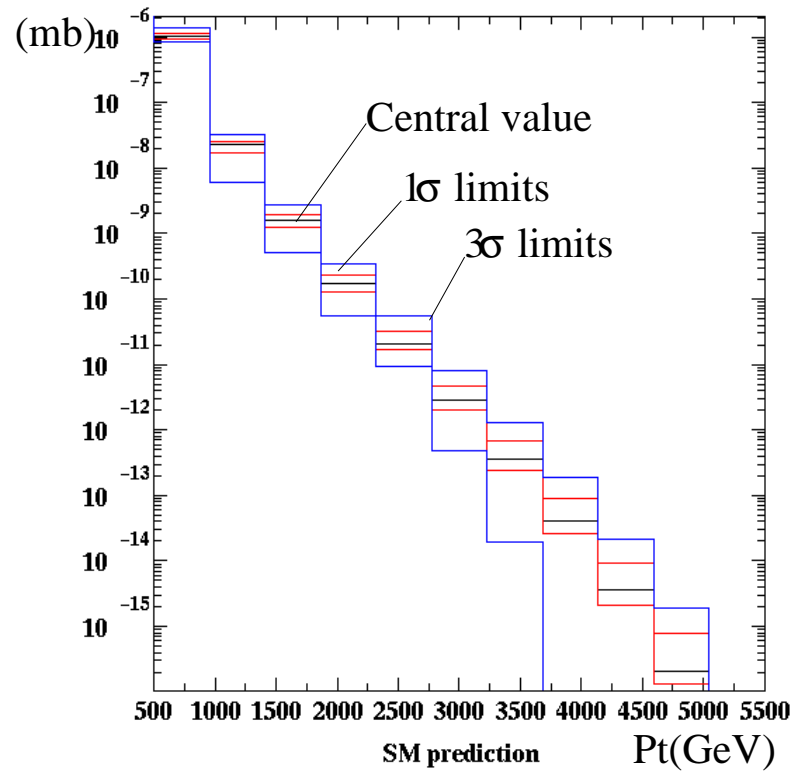


Figure 6: *Standard Model di-jets cross section prediction and uncertainties zone at  $1\sigma$  and  $3\sigma$ .*



Table 1: *Upper limit in compactification scale reached by the sensitivity to extra-dimensions including and without including the proton structure uncertainties. The discovery potential is fixed for a value of the significance  $S > 5\sigma$ .*

	2 extra-dimensions	4 extra-dimensions	6 extra-dimensions
Theoretically	5 TeV	5 TeV	5 TeV
including PDF uncertainties	< 2 TeV	< 3 TeV	< 4 TeV

### 3.3 Proton structure uncertainties components

To understand the source of the large uncertainties above, we show in figure (7) the contributions to the  $parton + parton \rightarrow parton + parton$  cross section depending if the initial partons are quarks, gluons or both. Figure (7.b) shows that in the case of the quarks, the 40 PDFs predictions are confined close to the nominal prediction. This proves that the quark density functions are well known. This is not the case of the gluon density function. As shown in plots (7.c) and (7.d), when one or both of the initial partons are gluons. It appears that gluons dominates the large uncertainties in the predictions.

### 3.4 Impact of the proton structure on the extra-dimensions sensitivity

The Standard Model prediction zone have been established in the previous section and the main PDF source of uncertainties is understood. To illustrate the impact of PDF uncertainties on the extra-dimensions sensitivity, extra-dimensions predictions are compared to the Standard Model prediction zone. When we increase the compactification scale  $M_c$  the extra-dimensions predictions go towards the Standard Model zone and falls into this latter for  $M_c > 2$  TeV, see figure (8). In this case, an extra-dimensions prediction is considered as a Standard Model prediction with a new set of PDFs because it is sitted in the Standard Model prediction zone. Thus, even if the extra-dimensions exist, the corresponding di-jets cross section measured in this uncertainties zone is compatible with the Standard Model prediction and one can not confirm their existence. This fact attenuates the extra-dimensions discovery potential. The corresponding sensitivity calculations are given below.

## 4 Results

Including the PDF uncertainties, the extra-dimensions significance is estimated by comparing the extra-dimensions predictions to the lower limit of the Standard Model zone because the extra-dimensions effect is to cancel the di-jets signal. The statistical significance  $S$  is computed for the first year of the LHC high luminosity, *ie*,  $100 \text{ fb}^{-1}$ . This is given by:

$$S = \frac{N_{low}^{SM} - N_{(\delta, M_c)}^{XD}}{\sqrt{N_{low}^{SM}}}, \quad (9)$$

where  $N_{low}^{SM}$  is the lower number of events predicted by the Standard Model.  $N_{(\delta, M_c)}^{XD}$  is the number of the events predicted by the extra-dimensions model using parameters  $(\delta, M_c)$ .

Figure (9) and table (1) show the results of the significance of extra-dimensions existance using the references <sup>3,4</sup> model. For different extra-dimensions  $(\delta, M_c)$  parameters, we see that

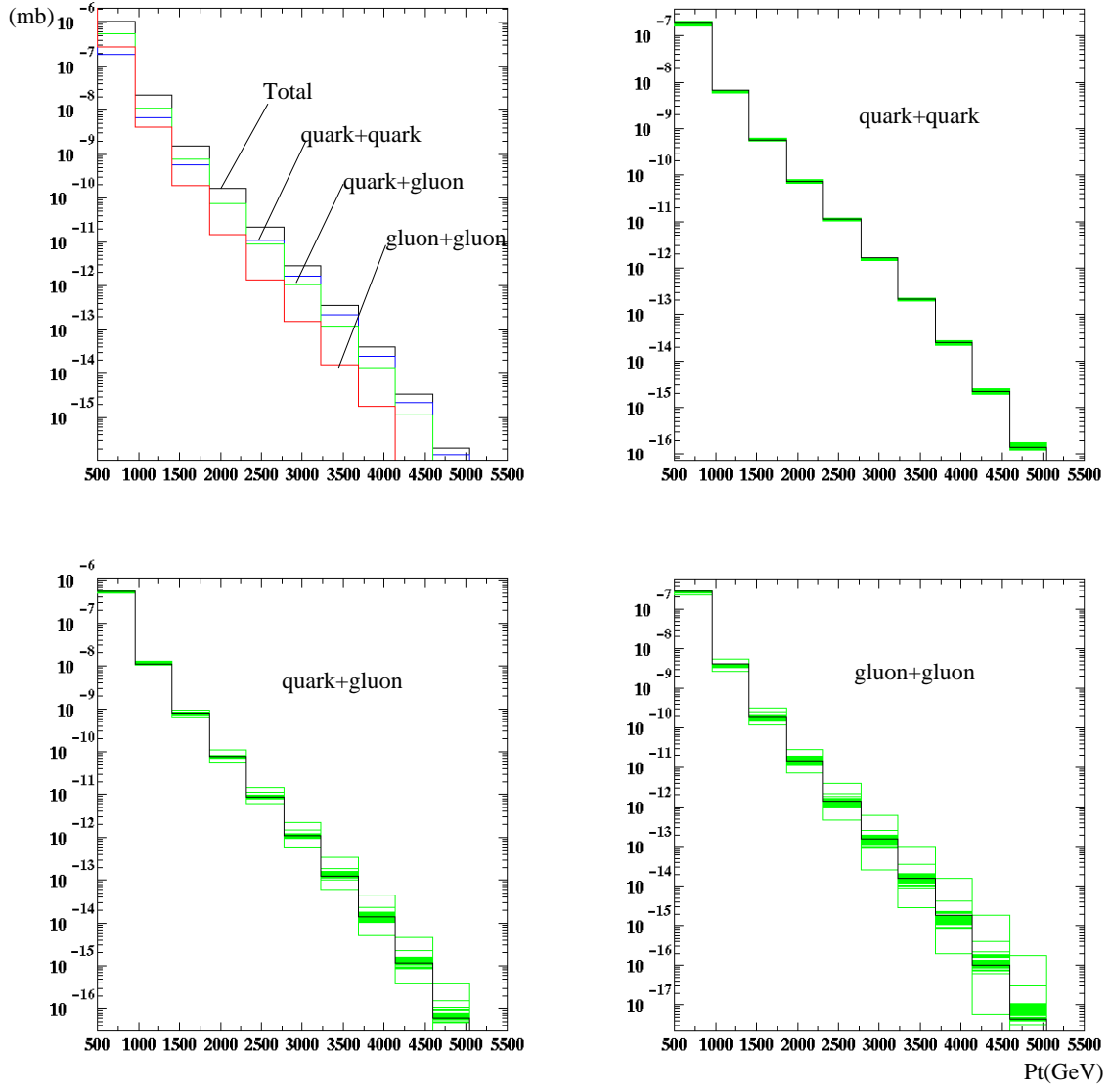


Figure 7: *Standard Model: (up left) different contributions to the total di-jet cross section according to the nature of the initial partons. (Up right) prediction using CTEQ6M and error PDFs when both of the initial partons are quarks. (Down left) one of the initial partons is a gluon and the other is a quark. (Down right) both of the partons are gluons.*

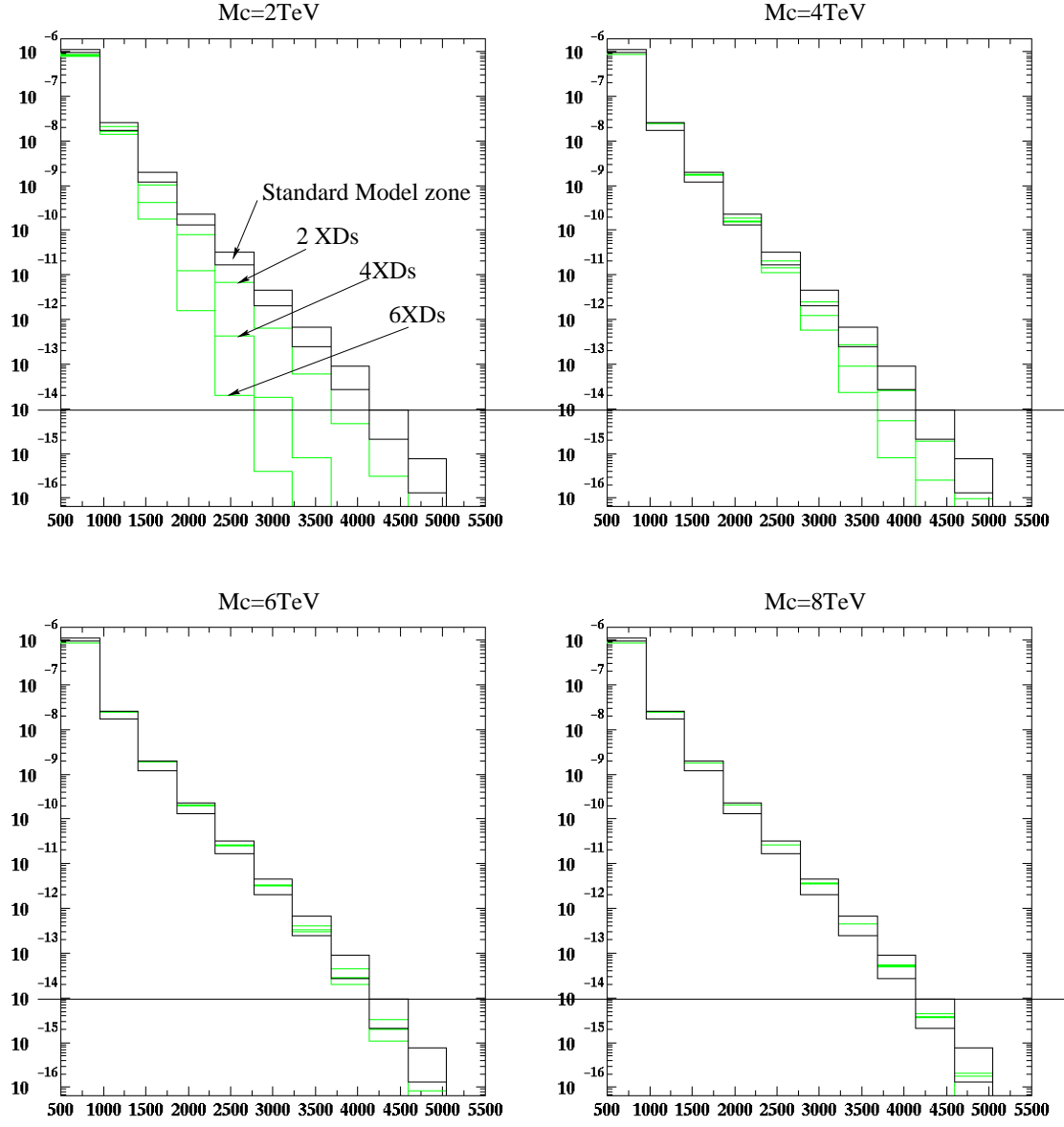


Figure 8: *Standard Model and extra-dimensions predictions comparison: The extra-dimension predictions are well separated from the Standard Model uncertainties zone for  $M_c = 2$  TeV (up left). By increasing the compactification scale, some of those predictions falls into the Standard Model band and may be considered as Standard Model prediction with a new PDF fit.*

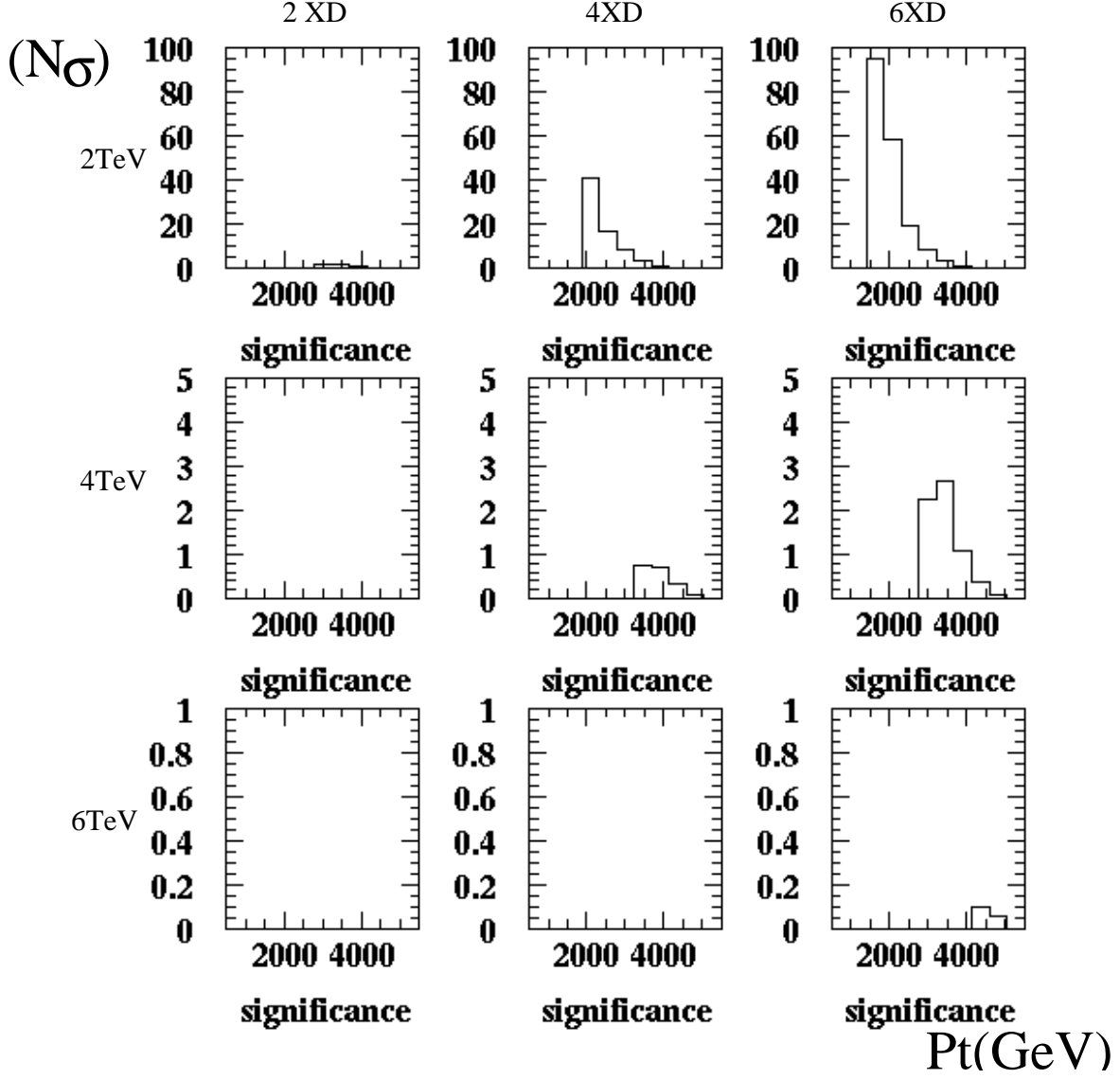


Figure 9: *Significance of extra-dimensions existence for different numbers of extra-dimensions and different compactification scales. With  $\delta = 2$  extra-dimensions, the significance is lower than  $5\sigma$ s (left column). When we fix the significance sensitivity to more than  $5\sigma$ , this latter is up to 2 TeV in compactification scale for  $\delta = 4$  extra-dimensions (middle column) and between 2 and 4 TeV in compactification scale for  $\delta = 6$  extra-dimensions (right column).*

in the case of  $\delta = 2$ , sensitivity is completely lost, ie, the reached upper limit of  $M_c$  is lower than 2 TeV. The discovery potential fixed at  $S > 5\sigma$  reaches  $M_c=2$  or 3 TeV for  $\delta = 4$  or 6 extra-dimensions . Theoretically<sup>5</sup>, sensitivity reaches  $M_c=5$  TeV for all the  $\delta$  values in the same scenario. So, the ignorance of the proton structure degrades significantly the discovery of the extra-dimensions using the di-jet cross section measurement.

## 5 Conclusion

The discovery of extra-dimensions through RGE violation needs a good understanding of QCD effects at LHC. The analysis presented here gives as a first result the Standard Model di-jet cross section prediction zone which is an extra-dimensions model independent result. It shows also as a second result a significant decrease of the extra-dimensions discovery potential from  $M_c = 5$  TeV to below 2 to 3 TeV depending on the number of extra-dimensions . Consequently, using di-jets cross section to search for extra-dimensions suffers from the ignorance of the proton structure. More complicated strategies to recover an important part of the sensitivity have to be developed. An example of these strategies could be the investigation of the ratio 2 jets/3 jets where we can expect a lower sensitivity to the PDF uncertainties.

High  $x$  gluon is responsible of the largest part of the ignorance of the proton structure. So, it is very important to do QCD analysis including LHC data to investigate the proton structure and to allow LHC experiments to look for new physics.

## Acknowledgments

We thank very much Joey Huston and Daniel Stamp from CTEQ collaboration for many interesting discussions.

## References

1. N. Arkani-Hamed, S. Dimopoulos and G. Dvali, Phys. Lett. **B429**, 263 (1998) [hep-ph/9803315].
2. L. Randall and R. Sundrum, Phys. Rev. Lett. **83**, 3370 (1999) [hep-ph/9905221].
3. K. R. Dienes, E. Dudas and T. Gherghetta, Phys. Lett. B **436**, 55 (1998) [hep-ph/9803466].
4. K. R. Dienes, E. Dudas and T. Gherghetta, Nucl. Phys. B **537**, 47 (1999) [hep-ph/9806292].
5. C. Balázs, B. Laforge, *Probing TeV-scale gauge unification by hadronic collisions*, Phys Let **B 525** (2002) 219.
6. M. Masip, Phys. Rev. D **62**, 105012 (2000) [hep-ph/0007048].
7. J. Pumplin, D.R. Stump, J. Huston, H.L. Lai, P. Nadolsky, W.K. Tung JHEP **0207** (2002) 012, hep-ph/0201195
8. universal PDF interface. It replaces the Pdffib  
<http://vircol.fnal.gov/>